Mixed-state quantum transport in correlated spin networks

Ashok Ajoy* and Paola Cappellaro†

Department of Nuclear Science and Engineering, Massachusetts Institute of Technology, Cambridge, Massachusetts 02139, USA

(Received 22 February 2012; published 5 April 2012)

Quantum spin networks can be used to transport information between separated registers in a quantum-information processor. To find a practical implementation, the strict requirements of ideal models for perfect state transfer need to be relaxed, allowing for complex coupling topologies and general initial states. Here we analyze transport in complex quantum spin networks in the maximally mixed state and derive explicit conditions that should be satisfied by propagators for perfect state transport. Using a description of the transport process as a quantum walk over the network, we show that it is necessary to phase-correlate the transport processes occurring along all the possible paths in the network. We provide a Hamiltonian that achieves this correlation and use it in a constructive method to derive engineered couplings for perfect transport in complicated network topologies.

DOI: 10.1103/PhysRevA.85.042305 PACS number(s): 03.67.Ac, 03.67.Hk

I. INTRODUCTION

In the quest toward a scalable quantum computer [1], a promising model comprises distributed computing units connected by passive wires that transmit quantum information [2–6]. This architecture would provide several advantages, since the wires require no or limited control, easing the fabrication requirements and improving their isolation from the environment. For simpler integration in a solid-state architecture, the wires can be composed of spins. Following seminal work by Bose [7], which showed that spin chains enable transporting quantum states between the ends of the chain, the dynamics of quantum-state transfer has been widely studied (see Ref. [8] for a review) and protocols for improving the fidelity by coupling engineering [9–16], dual-rail topologies [17], and active control on the chain spins [18] or on the end spins only [19–22] have been proposed. Recently these studies have been extended to mixed-state spin chains [23–27], which are more easily obtained in high-temperature laboratory settings—making them important protagonists in practical quantum computing. A further challenge to experimental implementation of quantum transport is the lack of chains with the desired coupling strengths, since coupling engineering is limited by fabrication constraints and by the presence of long-range interactions. These challenges highlight the need for a systematic study of mixed-state transport in quantum systems beyond chains, including more complex network topologies. These topologies reflect more closely actual experimental conditions as well as systems occurring in nature. For example, there is remarkable recent evidence [28,29] that coherent quantum transport may be the underlying reason for the high efficiency (of over 99%) of photosynthetic energy transfer [30].

To derive explicit conditions for perfect transport we quantify geometric constraints on the unitary propagator that drives transport in an arbitrary network. As a consequence, we find that transferring some mixed states in a network in general requires fewer conditions than pure-state transfer. Transport conditions for pure states have been previously quantified [31]; however, our method—relying on decomposing the propagator in orthogonal spaces—is fundamentally different and more suitable for mixed states.

Perfect transport occurs when the bulk of the network acts like a lens to *focus* transport to its ends. To make this physical picture more concrete, we describe mixed-state transport as a continuous quantum walk over the network [32–34] that progressively populates its nodes. Through this formalism, we derive constructive conditions on the Hamiltonian that result in the *correlation* of transport processes through different possible paths in the network. The correlation of transport processes leads to their constructive interference at the position of the two end spins, giving perfect transport. While similar walk models have been applied to coherent transfer before (see [35] for a review), our work provides an extension to transport involving mixed states.

The insight gained by describing quantum transport as correlated quantum walks can be used to construct larger networks where perfect transport is possible. Here we show a strategy to achieve this goal by engineering the coupling strengths between different nodes of the network to construct *weighted* spin networks that support perfect mixed-state transport. Feder [36] had considered a similar problem for pure states by mapping the quantum walk of N spinor bosons to a single particle; this has been extended in more recent work [37–39]. Here we find far more relaxed weighting requirements for mixed-state transport, thanks in part to a fermionic instead of bosonic mapping. In turn, this could ease the fabrication requirements for coupling engineering.

The paper is organized as follows. In Sec. II we define the problem of mixed-state transport. Section III provides the geometric conditions on the propagator for perfect transport in arbitrary networks. We finally present in Sec. IV the quantum-walk formalism, which allows the correlation of transport processes over different paths and the construction of families of weighted networks that support perfect transfer.

II. TRANSPORT IN MIXED-STATE NETWORKS

Consider an N-spin network $\mathcal{N}$, whose vertices (nodes) $\mathcal{V}$ represent spins and whose edges $\mathcal{E} = \{\alpha_{ij}\}$ describe the couplings between spins i and j (see Fig. 1). The system dynamics is governed by the Hamiltonian $H = \sum_{i<j} \alpha_{ij} H_{ij}$, where H_{ij} is the operator form of the interaction. In the

*ashokaj@mit.edu
†pcappell@mit.edu

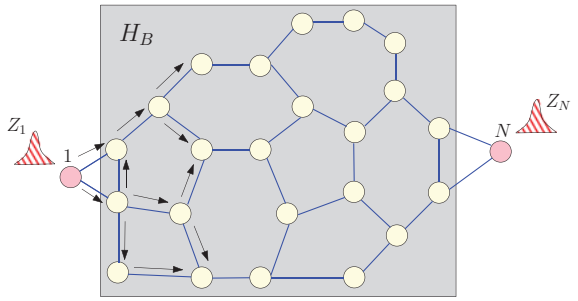

FIG. 1. (Color online) Transport in a spin network. The network edges represent the interaction among spins (nodes). The pink (dark) nodes represent the *end* spins between which transport should occur. The shaded region comprising yellow (light) nodes is the *bulk* network H_B. An initial polarization packet (hatched) is prepared on spin 1 and allowed to propagate on the network through various possible paths (arrows). For perfect transport, the polarization refocuses at spin N.

most general case, a spin of $\mathcal{N}$ may be coupled to several others, for instance, in a dipolar coupled network, $\alpha_{ij} \sim 1/r_{ij}^3$ is a function of the distance between the spins in the network.

We assume that we can identify two nodes, labeled 1 and N, that we can (partially) control and read out, independently from the "bulk" of the network, and thus act as the "end" spins between which transport will occur. The rest of the spins in the network can at most be manipulated by collective control. This also imposes restrictions on the network initialization [24–26]. To relax the requirements for the network preparation, we assume to work in the infinite-temperature limit [25]—a physical setting easily achievable for many experimental systems—where the bulk spins are in the maximally mixed state, $\rho \propto \mathbb{1}$. We will then consider the transport of a slight excess polarization from node 1 to node N. The initial state is $\rho_i \sim (\mathbb{1} + \delta Z_1)$, where Z_1 is the Pauli matrix acting on spin 1 and $\delta \ll 1$ denotes the polarization excess. Since only the traceless part of the density matrix evolves in time, we will monitor the transport from $\rho_i^\Delta = Z_1$ to a desired final state $\rho_f^\Delta = Z_N$. The *fidelity* of the transport process is then defined as $F(t) = \mathrm{Tr}[\rho^\Delta(t) Z_N]/\mathrm{Tr}[Z_1^\dagger Z_1]$, with $\rho^\Delta(t) = U(t)\rho_i^\Delta U^\dagger(t)$ being the evolved state.

The polarization behaves like a wave packet traveling over the network $\mathcal{N}$ [40,41]. In most cases, the Hamiltonian H drives a rapidly dispersive evolution, where the wave packet quickly spreads out into many-body correlations among the nodes of $\mathcal{N}$, from which it cannot be recovered [34]. This is, for example, the case of evolution under the naturally occurring dipolar Hamiltonian, which induces a fast decay of the spin polarization as measured in solid-state NMR, even if many-body correlations can be detected at longer times [42].

In order to drive a dispersionless transport, thus ensuring perfect fidelity, the network Hamiltonian should satisfy very specific conditions. In this paper we will investigate these conditions by answering the questions: (i) What are the possible operator forms of the Hamiltonian H_{ij} for dispersionless transport? What are the (ii) coupling topologies and (iii) strengths α_{ij} that support perfect transport?

III. CONDITIONS FOR PERFECT TRANSPORT

A. Fidelity of mixed-state transport

The condition for perfect transport, $F = 1$, can be expressed in a compact form by using the product-operator (PO) basis [43]. For the N-spin network system there are 2^{2N} basis elements,

$$\mathbf{B} = \mathbf{B}_1 \otimes \mathbf{B}_{\mathrm{bulk}} \otimes \mathbf{B}_N = \{\mathbb{1}, X_1, Y_1, Z_1, X_2, \ldots, X_1X_2, \ldots, Z_1Z_2, X_1X_2X_3, \ldots, Z_1Z_2\cdots Z_{N-1}Z_N\}, \quad (1)$$

where $\mathbf{B}_{1,N}$ and $\mathbf{B}_{\mathrm{bulk}}$ are the bases for the end and the bulk spins, respectively.

Using the PO basis, the propagator $U(t) = e^{-iHt}$ can be represented by a vector $|U\rangle = [c_{B_1}, c_{B_2}, \ldots, c_{B_{4^N}}]^T$ in the 2^{2N}-dimensional Hilbert-Schmidt (HS) operator space spanned by $\mathbf{B}$ [44]:

$$U(t) = \sum_i c_{B_i}(t) B_i \quad \text{with} \quad c_{B_i} = \frac{\mathrm{Tr}(B_i^\dagger U)}{\mathrm{Tr}(B_i^\dagger B_i)}.$$

From an initial state with a polarization excess on spin 1, $\rho_i^\Delta = Z_1$, the system evolves to

$$\rho_f^\Delta = U\rho_i^\Delta U^\dagger = \sum_{i,j} c_{B_i} c_{B_j}^* B_i Z_1 B_j\,, \quad (2)$$

yielding the transport fidelity to spin N

$$F = \frac{1}{\mathrm{Tr}(Z_1^\dagger Z_1)} \mathrm{Tr}\left[\sum_{i,j} c_{B_i}^* c_{B_j} B_i Z_1 B_j Z_N\right] = \sum_i c_{B_i} c_{B_j}^* \quad \text{with} \quad B_j = \pm Z_1 Z_N B_i \quad \text{for} \quad [B_i, Z_N]_\mp = 0. \quad (3)$$

The last equation follows from the property that all elements of $\mathbf{B}$, except $\mathbb{1}$, are traceless.

The fidelity derived in Eq. (3) has a simple form in the HS space. Note that, in this operator space, the product $B_i U$ is a linear transformation $\mathbf{T} : |U\rangle \to \hat{P}_{B_i}|U\rangle$, where $\hat{P}_{B_i}$ is a permutation matrix corresponding to the action of B_i [44] (here and in the following we denote operators in the HS space by a caret). The unitarity of U yields the conditions

$$\|U\| = \langle U|U\rangle = 1, \quad \langle U|\hat{P}_{B_i}|U\rangle = 0, \quad B_i \neq \mathbb{1}. \quad (4)$$

Let us partition the HS space into two subspaces $\mathcal{G}$ and $\widetilde{\mathcal{G}}$, spanned by the bases G and $\widetilde{G}$,

$$G = \mathbf{B}_1 \otimes \mathbf{B}_{\mathrm{bulk}} \otimes \{\mathbb{1}, Z_N\}, \quad \widetilde{G} = \mathbf{B}_1 \otimes \mathbf{B}_{\mathrm{bulk}} \otimes \{X_N, Y_N\},$$

and note that all elements of G commute with Z_N, while all elements of $\widetilde{G}$ anticommute with Z_N. We will label by superscripts $\mathcal{G}$ and $\widetilde{\mathcal{G}}$ the projections of operators in these subspaces. Using this partition, we can simplify the expression for the fidelity of Eq. (3) to obtain

$$F = \langle U|\hat{P}_{Z_1Z_N}\hat{P}_R|U\rangle, \quad (5)$$

where $\hat{P}_R$ is a reflection about $\mathcal{G}$ and $\hat{P}_{Z_1Z_N}$ is block diagonal in the $\{G, \widetilde{G}\}$ basis (since $Z_1Z_N \in \mathcal{G}$):

$$\hat{P}_R = \begin{bmatrix} \mathbb{1}^{\mathcal{G}} & 0 \\ 0 & -\mathbb{1}^{\widetilde{\mathcal{G}}} \end{bmatrix}, \quad \hat{P}_{Z_1Z_N} = \begin{bmatrix} \hat{P}^{\mathcal{G}}_{Z_1Z_N} & 0 \\ 0 & \hat{P}^{\widetilde{\mathcal{G}}}_{Z_1Z_N} \end{bmatrix}. \quad (6)$$

Rewriting the fidelity as the inner product between two vectors, $F = \langle(\hat{P}_{Z_1Z_N}U)|\hat{P}_R U\rangle$, provides a simple geometric

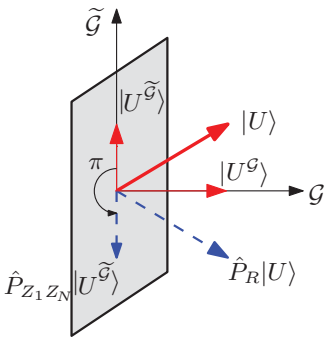

FIG. 2. (Color online) Geometric interpretation of the condition for maximum $Z_1 \to Z_N$ transport fidelity. The unitary U is represented as a vector $|U\rangle$ (red thick arrow) in the HS space, with components $|U^{\mathcal{G}}\rangle$ and $|U^{\widetilde{\mathcal{G}}}\rangle$ in the subspaces $\mathcal{G}$ (represented by an axis) and $\widetilde{\mathcal{G}}$ (represented by the shaded gray plane). $\hat{P}_R|U\rangle$ (blue dashed arrow) is the reflection of $|U\rangle$ about the $\mathcal{G}$ axis. Maximum fidelity occurs only when $\hat{P}_{Z_1Z_N}$ causes a π rotation of $|U^{\widetilde{\mathcal{G}}}\rangle$.

interpretation of the perfect transport condition, as shown in Fig. 2. The vector $\hat{P}_{Z_1Z_N}|U\rangle$ should be *parallel* to $\hat{P}_R|U\rangle$, which can be obtained if $\hat{P}_{Z_1Z_N}$ rotates $|U^{\widetilde{\mathcal{G}}}\rangle$ by an angle π, while leaving $|U^{\mathcal{G}}\rangle$ unaffected. Alternatively, since $\hat{P}_{Z_1Z_N}$ just describes a π rotation of the vector $|U\rangle$ about the Z_1Z_N axis, for perfect transport the rotation-reflection operation $\hat{S} = \hat{P}_{Z_1Z_N}\hat{P}_R$ should be a *symmetry* operation for $|U\rangle$.

From Eq. (4) we have $\langle U|\hat{P}_{Z_1Z_N}|U\rangle = 0$ and using Eq. (5) we can derive explicit conditions to be satisfied by the propagator to achieve perfect transport, $F = 1$:

$$\langle U^{\mathcal{G}}|\hat{P}^{\mathcal{G}}_{Z_1Z_N}|U^{\mathcal{G}}\rangle + \langle U^{\widetilde{\mathcal{G}}}|\hat{P}^{\widetilde{\mathcal{G}}}_{Z_1Z_N}|U^{\widetilde{\mathcal{G}}}\rangle = 0, \tag{7}$$

$$\langle U^{\mathcal{G}}|\hat{P}^{\mathcal{G}}_{Z_1Z_N}|U^{\mathcal{G}}\rangle - \langle U^{\widetilde{\mathcal{G}}}|\hat{P}^{\widetilde{\mathcal{G}}}_{Z_1Z_N}|U^{\widetilde{\mathcal{G}}}\rangle = 1, \tag{8}$$

which simplify to

$$\langle U^{\mathcal{G}}|\hat{P}^{\mathcal{G}}_{Z_1Z_N}|U^{\mathcal{G}}\rangle = -\langle U^{\widetilde{\mathcal{G}}}|\hat{P}^{\widetilde{\mathcal{G}}}_{Z_1Z_N}|U^{\widetilde{\mathcal{G}}}\rangle = \tfrac{1}{2}. \tag{9}$$

When is this equation satisfied? By symmetry, it happens when $\|U^{\mathcal{G}}\| = \|U^{\widetilde{\mathcal{G}}}\| = 1/2$, and $|U^{\mathcal{G}}\rangle$ and $|U^{\widetilde{\mathcal{G}}}\rangle$ are (up to a phase) eigenvectors of $\hat{P}^{\mathcal{G}}_{Z_1Z_N}$ and $\hat{P}^{\widetilde{\mathcal{G}}}_{Z_1Z_N}$ with eigenvalues ± 1, respectively:

$$\hat{P}^{\mathcal{G}}_{Z_1Z_N}|U^{\mathcal{G}}\rangle = +|U^{\mathcal{G}}\rangle; \quad \hat{P}^{\widetilde{\mathcal{G}}}_{Z_1Z_N}|U^{\widetilde{\mathcal{G}}}\rangle = -|U^{\widetilde{\mathcal{G}}}\rangle. \tag{10}$$

To enable perfect transport, $|U\rangle$ must thus have an equal projection on the two subspaces $\mathcal{G}$ and $\widetilde{\mathcal{G}}$, as shown geometrically in Fig. 2. Also, intuitively from the symmetry operation $\hat{S}$, all components of $|U\rangle$ lying on the plane $\mathcal{G}$ should be rotationally symmetric with respect to Z_1Z_N, while components of $|U\rangle$ lying on the plane $\widetilde{\mathcal{G}}$ should have reflection symmetry about Z_1Z_N.

Note that Eq. (10) imposes fairly weak constraints on the transport unitaries, as opposed to the constraints for pure-state transport [31,45]. In particular Eq. (10) provides no explicit constraint on the bulk of the network. For example, the two propagators

$$\begin{aligned} U_1 &= B_{\text{bulk}}(\mathbb{1} \pm Z_1Z_N) + B'_{\text{bulk}}(X_1X_N \pm Y_1Y_N), \\ U_2 &= B_{\text{bulk}}(\mathbb{1} \pm Z_1Z_N) + B'_{\text{bulk}}(X_1Y_N \mp Y_1X_N), \end{aligned} \tag{11}$$

with B_{bulk} and B'_{bulk} arbitrary equi-norm operators ($\in \text{span}\{\mathbf{B}_{\text{bulk}}\}$) acting on the bulk, support perfect transport. Other propagators can be obtained thanks to an invariance property that we present in the next section. More generally, in Appendix A we explicitly provide a prescription to construct classes of unitaries for perfect mixed-state transport.

B. Invariance of transport Hamiltonians

The fidelity F in Eq. (3) is invariant under a transformation $U' = VU$, where V is unitary and commutes with $\hat{S}$, that is,

$$\left[\hat{V}, \hat{P}_{Z_1Z_N}\hat{P}_R\right] = 0. \tag{12}$$

This invariance can be used to construct Hamiltonians that support perfect transport starting from known ones. Consider a Hamiltonian H that generates the transport evolution $U = \exp(-iHt)$. Then the transport driven by H is *identical* to that generated by the Hamiltonian $H' = V^\dagger HV$, where V satisfies Eq. (12).

The authors of Ref. [46] proved similar symmetry requirements for Hamiltonians that transport pure states; here, however, we derived these Hamiltonian properties just from the geometric conditions on U. In Ref. [47] a similar problem was treated, defining classes of Hamiltonians that perform the same action on a state of interest. A special case of this result was used in Ref. [23] to study transport in a mixed-state spin chain driven either by the nearest-neighbor coupling isotropic XY Hamiltonian

$$H_{XY} = \sum_i \alpha_i T^+_{ii+1} \quad \text{with} \quad T^+_{ij} = (S^+_i S^-_j + S^-_i S^+_j) \tag{13}$$

or by the double-quantum (DQ) Hamiltonian

$$H_{\text{DQ}} = \sum_i \alpha_i D^+_{ii+1} \quad \text{with} \quad D^+_{ij} = (S^+_i S^+_j + S^-_i S^-_j), \tag{14}$$

with $S^\pm_j = \frac{1}{2}(X_j \pm iY_j)$. The unitary operator relating the two Hamiltonians, $V = \prod_{k'} X_{k'}$, where the product k' extends over all even *or* odd spins, does indeed satisfy Eq. (12).

C. Quantum-information transport via mixed-state networks

The requirements for perfect transport [Eq. (10)] can be easily generalized to the transport between any two elements of $\mathbf{B}$, say from $\mathcal{I}$ to $\mathcal{F}$. One has simply to appropriately construct the subspaces $\mathcal{G}$ and $\widetilde{\mathcal{G}}$ and the corresponding permutation operator $\hat{P}_{\mathcal{I}\mathcal{F}}$.

One could further consider under which conditions this transport (for example, $X_1 \to X_N$) can occur *simultaneously* with the $Z_1 \to Z_N$ transport already considered. More generally, the simultaneous transfer of operators forming a basis for $\mathbf{B_1}$ would enable the transport of quantum information [10,25] via a mixed-state network. The unitary U should now not only be symmetric under $\hat{S}$, but also under a similar operator derived for X_1X_N. The requirements on U thus become more stringent and only a special case of the propagators constructed in Eq. (A3) in Appendix A is allowed,

$$U = B_{\text{bulk}}(\mathbb{1} \pm Z_1Z_N + X_1X_N \pm Y_1Y_N). \tag{15}$$

This is exactly a SWAP operation (up to a phase) between the end spins, which can also lead to a transfer of arbitrary

pure states between 1 and N. Therefore, we find that perfect transport of noncommuting mixed states between the end spins also allows transport in pure-state networks. We note that quantum information could be encoded in multispin states [25,48] that satisfy proper symmetry conditions and thus do not impose additional conditions on the transport propagators.

D. Which Hamiltonians support mixed-state transport?

It would be interesting to determine which Hamiltonians can generate propagators $|U(t)\rangle = \exp(-i\hat{H}t)|\mathbb{1}\rangle$ for perfect transport. Unfortunately, deriving requirements for the Hamiltonian from the conditions on the unitaries is nontrivial; however, as we show below, one can still extract useful information.

A general Hamiltonian can be decomposed as $H = H^{\mathcal{G}} + H^{\widetilde{\mathcal{G}}}$, where $H^{\mathcal{G},\widetilde{\mathcal{G}}}$ lie in the subspaces $\mathcal{G}$ and $\widetilde{\mathcal{G}}$, respectively. We cannot set $H = H^{\mathcal{G}}$ since the Hamiltonian does need to have a component that is noncommuting with the target operator (Z_N) in order to drive the transport. If $H = H^{\widetilde{\mathcal{G}}}$, odd powers of H are in $\widetilde{\mathcal{G}}$, while even powers of H belong to $\mathcal{G}$. Then the propagator has contributions from $|U^{\mathcal{G}}\rangle$ and $|U^{\widetilde{\mathcal{G}}}\rangle$ with

$$\begin{aligned} |U^{\mathcal{G}}\rangle &= |\mathbb{1}\rangle + \frac{(it)^2}{2!}\hat{H}|H\rangle + \frac{(it)^4}{4!}\hat{H}^3|H\rangle + \cdots, \\ |U^{\widetilde{\mathcal{G}}}\rangle &= it|H\rangle + \frac{(it)^3}{3!}\hat{H}^2|H\rangle + \cdots. \end{aligned} \tag{16}$$

We can demonstrate that in this case the Hamiltonian must satisfy two conditions to drive perfect transport. First, the "vector" form of the Hamiltonian must be an eigenstate of $\hat{P}_{Z_1Z_N}$, $\hat{P}_{Z_1Z_N}|H\rangle = -|H\rangle$, which ensures that the second equation in (10) is trivially satisfied, as $\hat{P}_{Z_1Z_N}|U^{\widetilde{\mathcal{G}}}\rangle = -|U^{\widetilde{\mathcal{G}}}\rangle$. Second, since we have

$$\hat{P}_{Z_1Z_N}|U^{\mathcal{G}}\rangle = |Z_1Z_N\rangle + \frac{(it)^2}{2!}\hat{H}|H\rangle + \frac{(it)^4}{4!}\hat{H}^3|H\rangle + \cdots,$$

the first equation in (10) implies that $H^{2n} = \frac{1}{2}(\mathbb{1} - Z_1Z_N)$ for any n.

These conditions are for example satisfied by the XY-like Hamiltonian $H = B_{\text{bulk}}T^+_{1N}$, where B_{bulk} is any operator acting on the bulk. In this case, at $t = \pi/4$, all conditions in Eq. (10) are satisfied and perfect transport is achieved. Indeed, the XY Hamiltonian has been widely studied for quantum transport [7,9] and it is interesting that we could derive its transport properties solely by the symmetry conditions on the propagator.

A Hamiltonian $H = H^{\widetilde{\mathcal{G}}}$ with support only in $\widetilde{\mathcal{G}}$ is, however, a very restrictive case as it refers to the situation where all nodes of the network are connected to N. Hamiltonians with support in both subspaces are more experimentally relevant, as they correspond to a common physical situation, where the ends of the network are separated in space and direct interaction between them is zero or very weak. In the following, we will consider this more general situation, although restricting the study to XY Hamiltonians in order to derive conditions for perfect transport.

IV. PERFECT TRANSPORT IN NETWORKS: CORRELATED QUANTUM WALKS

In the following, we will consider the network $\mathcal{N}$ to consist of spins that are coupled by XY-like interaction, $\{T^+_{ij}\}$. We focus on this interaction since it has been shown that with appropriate *engineered* coupling strengths, $\alpha_{ij} \propto \sqrt{i(N-i)}\delta_{j,i+1}$, the XY-Hamiltonian can support perfect transport in linear spin chains (see, e.g., [10–12,49]). Thanks to the invariance property described in Sec. III B, this analysis applies to a much broader class of Hamiltonians, in particular to the DQ Hamiltonian.

We assume that the end spins of $\mathcal{N}$ are not directly coupled; thus transport needs to be mediated by the bulk of the network. The simplest such topology is a Λ-type configuration where the end spins are coupled to a single spin in the bulk. The Hamiltonian $\Lambda_j = (T^+_{1j} + T^+_{jN})/\sqrt{2}$, where j is a spin in the bulk, is enough to drive this transport. In this case, $(\Lambda^2_j)^n = \Lambda^2_j \; \forall \; n$, and hence the propagator is

$$U = \exp(-iHt) = \mathbb{1} + [\cos(t) - 1]H^2 - i\sin(t)H, \tag{17}$$

where $H^2 = 1/2[(T^+_{1j})^2 + (T^+_{jN})^2 + T^+_{1N}]$. Since $(\mathbb{1} - 2H^2)$ has the form of U_3 in Eq. (A3), setting $t = \pi$ ensures $U = U_3$, yielding perfect transport. This is an expected result, since this simple Λ network is just a three-spin linear chain. This result can be extended to longer chains, as long as engineered couplings ensure that the resulting Hamiltonian is mirror symmetric [10,16,45].

A different situation arises when there is more than one transport *path* possible, that is, the end spins are coupled to more than one spin in the bulk with a Hamiltonian $H = \sum_{j\in\text{bulk}} \alpha_j \Lambda_j$. For example, Fig. 3 depicts a network similar to the one considered in Refs. [26,50] where there are three Λ paths between the end spins. Even if each path *individually* supports perfect transport, evolution along different paths may not be *correlated*, leading to destructive interference and reducing the fidelity (see Fig. 3).

Perfect fidelity can be achieved only if different paths can be *collapsed* into a single "effective" one that supports perfect transport (Fig. 8). This strategy not only allows us to determine

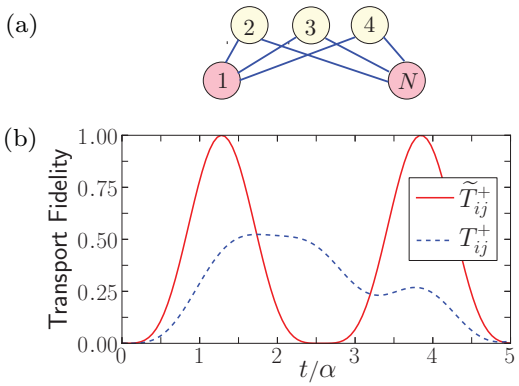

FIG. 3. (Color online) (a) Λ-type network with three Λ paths between the bulk and end spins and equal coupling strength α. (b) Transport fidelity as a function of normalized time for the Λ network coupled by the XY Hamiltonian T^+_{ij} (blue dashed) and the modified XY Hamiltonian $\widetilde{T}^+_{ij}$ (red solid). In the latter case, correlated quantum walks lead to perfect transport.

if an Hamiltonian can support perfect transport, but also gives a recipe to build allowed Hamiltonians, by combining simpler networks known to support perfect transport into more complex ones.

To this end, we use the fact that linear chains enable perfect transport with appropriate engineered couplings. Our first step will then give conditions under which two chains of the same length (with end spins in common) can be combined. To obtain these conditions, we describe the evolution of the spin polarization as a quantum walk over the operators in the network [33,34]. This description reveals the need to correlate the parallel paths over the network, in order to achieve a constructive refocusing of the polarization at the other end of the network. We then generalize the conditions by a recursive construction to quite general networks.

A. Transport as a quantum walk over $\mathcal{N}$

We describe the transport evolution as a quantum walk over the network, which progressively populates operators in the HS space. This process of progressively populating different parts of the HS space upon continuous-time evolution under the Hamiltonian can be considered as a quantum *walk* [33,34,51]. We first expand the transport fidelity $F(t)$ [Eq. (5)] in a time series,

$$F(t) = \langle U_0|\hat{P}_{Z_1Z_N}\hat{P}_R|U_0\rangle - it\langle U_0|[\hat{H},\hat{P}_{Z_1Z_N}\hat{P}_R]|U_0\rangle + \frac{i^2t^2}{2!}\langle U_0|\big[\hat{H},\big[\hat{H},\hat{P}_{Z_1Z_N}\hat{P}_R\big]\big]|U_0\rangle + \cdots \quad (18)$$

with $|U_0\rangle = |\mathbb{1}\rangle$. Defining the nested commutators

$$\mathcal{C}_0 = \hat{P}_{Z_1Z_N}\hat{P}_R, \quad \mathcal{C}_n = [\hat{H},\mathcal{C}_{n-1}], \quad (19)$$

Eq. (18) takes the form

$$F(t) = \sum_{n=0}^{\infty}\frac{(it)^n}{n!}\langle\mathcal{C}_n\rangle, \quad (20)$$

where the expectation value is taken with respect to $|U_0\rangle$.

A large part of the Hamiltonian commutes with $\hat{P}_{Z_1Z_N}\hat{P}_R$ and can be neglected. We can isolate the noncommuting part by defining the operator $\hat{A}$ via the relationship

$$\big[\hat{H},\hat{P}_{Z_1Z_N}\hat{P}_R\big] = \hat{A}\hat{P}_{Z_1Z_N}\hat{P}_R. \quad (21)$$

The operator $\hat{A}$ and its nested commutators $\mathcal{C}_n^A = [\hat{H},\mathcal{C}_{n-1}^A]$ (with $\mathcal{C}_0^A = \hat{A}$) have a simple graphical construction. The commutation relations

$$[T_{ij}^+,T_{jk}^\pm] = -Z_jT_{ik}^\mp, \quad [T_{ij}^+,T_{kl}^+] = 0, \quad (22)$$

(see Fig. 4) can be used to provide a simple prescription to graphically determine the flip-flop terms in $\mathcal{C}_n^A$. For any two edges, one in $\mathcal{C}_{n-1}^A$ and one in H, that share a common node, $\mathcal{C}_n^A$ contains the edge required to complete the triangle between them. Thus, each higher-order in the commutation expansion creates a link between nodes in the network, progressively populating it. We will refer to the operators $\mathcal{C}_n^A$ as quantum-walk operators, since as we show below, the nested commutators $\mathcal{C}_n$ in Eq. (20) can be built exclusively out of them.

Consider the network of Fig. 5(a), with coupling strengths $\alpha_{ij} = 1$: $\hat{A}$ contains only the edges of $\mathcal{N}$ that connect to node 1, as represented by the red lines in Fig. 5(b).

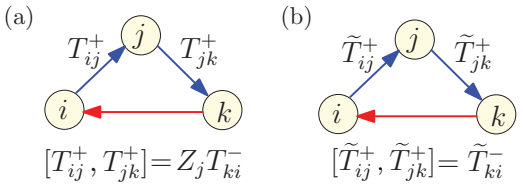

FIG. 4. (Color online) Graphical representation of commutators for (a) the *XY* and (b) the modified *XY* Hamiltonian. The commutator between two top legs (blue) of the directed graph is the third edge (red). In the case of the *XY* Hamiltonian, the commutator is conditioned on node j.

Figures 5(c) and 5(d) represent the higher-order commutators, with a red line linking two nodes denoting a term $T_{ij}^\pm$ between them. We note that the graphical construction only predicts the presence of a flip-flop term $T_{ij}^\pm$ linking two nodes in the commutator $\mathcal{C}_n^A$, while the explicit forms of the commutators are generally more complex, as shown in Table I, with additional appropriate weights for arbitrary coupling strengths α_{ij}. Still, as we now show, only the $T_{ij}^\pm$ terms are important to determine the fidelity, and the presence of a $T_{1N}^\pm$ term in the graphical series is an indication that transport can occur between the end nodes.

The commutators $\mathcal{C}_n$ can indeed be written in terms of the $\mathcal{C}_n^A$ nested commutators,

$$\mathcal{C}_n = \sum_{k=0}^{n-1}\binom{n-1}{k}\mathcal{C}_{n-1-k}^A\mathcal{C}_k, \quad (23)$$

yielding an expression for the fidelity containing only products of the nested commutators $\mathcal{C}_n^A$:

$$\mathcal{C}_n = \sum_{k_1=0}^{n-1}\sum_{k_2=0}^{k_1-1}\cdots\sum_{k_n=0}^{k_{n-1}-1}\binom{n-1}{k_1}\binom{k_1-1}{k_2}\cdots\binom{k_{n-1}-1}{k_n} \times \mathcal{C}_{n-k_1-1}^A\mathcal{C}_{k_1-k_2-1}^A\cdots\mathcal{C}_{k_{n-1}-k_n-1}^A\hat{P}_{Z_1Z_N}\hat{P}_R\,. \quad (24)$$

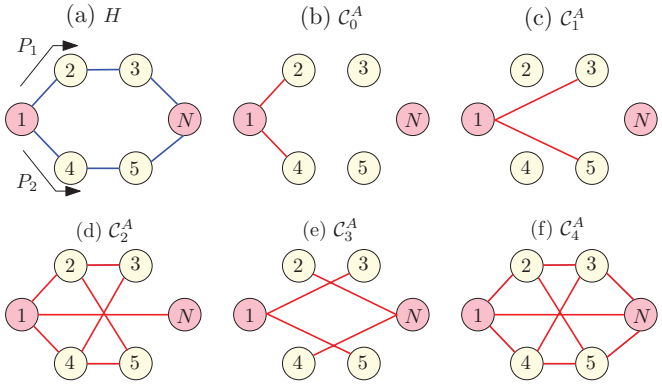

FIG. 5. (Color online) (a) A six-spin network with two paths P_1 and P_2 between the end spins. (b)–(f) represent graphically the successive orders of the quantum-walk operators $\mathcal{C}_n^A$: A red line linking two nodes indicates that there is a flip-flop term $T_{ij}^\pm$ between them, while path-dependent prefactors are not depicted. Once the walk has covered the entire network, successive orders in $\mathcal{C}_n^A$ reproduce $\mathcal{C}_3^A$ and $\mathcal{C}_4^A$. The explicit expressions for the commutators are shown in Table I.

TABLE I. Nested commutators $\mathcal{C}_n^A$ (walk operators) corresponding to the graphs in Fig. 5 if the edges represent the *XY* Hamiltonian or the modified *XY* Hamiltonian. In the first case, note the presence of path-dependent Z_j prefactors, which are absent if the modified *XY* Hamiltonian is used. This allows for the correlation of transport through parallel paths.

Walk operator	*XY* Hamiltonian	Modified *XY* Hamiltonian
$\mathcal{C}_0^A$	$T_{12}^+ + T_{14}^+$	$\widetilde{T}_{12}^+ + \widetilde{T}_{14}^+$
$\mathcal{C}_1^A$	$Z_2 T_{13}^- + Z_4 T_{15}^-$	$\widetilde{T}_{13}^- + \widetilde{T}_{15}^-$
$\mathcal{C}_2^A$	$T_{12}^+ - T_{23}^+ - Z_1 Z_2 T_{34}^+ + Z_2 Z_3 T_{1N}^+$	$\widetilde{T}_{12}^+ - \widetilde{T}_{23}^+ - \widetilde{T}_{34}^+ + \widetilde{T}_{1N}^+$
	$+T_{14}^+ - T_{45}^+ - Z_1 Z_4 T_{25}^+ + Z_4 Z_5 T_{1N}^+$	$+\widetilde{T}_{14}^+ - \widetilde{T}_{45}^+ - \widetilde{T}_{25}^+ + \widetilde{T}_{1N}^+$
$\mathcal{C}_3^A$	$(Z_4 Z_5 Z_N + 4Z_2) T_{13}^- + (Z_2 Z_3 Z_N + 4Z_4) T_{15}^-$	$5\widetilde{T}_{13}^- - 4\widetilde{T}_{2N}^-$
	$-2(Z_1 Z_4 Z_5 + Z_3) T_{2N}^- - 2(Z_1 Z_2 Z_3 + Z_5) T_{4N}^-$	$+5\widetilde{T}_{15}^- - 4\widetilde{T}_{4N}^-$
	$(4\mathbb{1} + Z_3 Z_4 Z_5 Z_N) T_{12}^+ + (4\mathbb{1} + Z_2 Z_3 Z_5 Z_N) T_{14}^+ + 9(Z_2 Z_3 + Z_4 Z_5) T_{1N}^+$	$5\widetilde{T}_{12}^+ + 5\widetilde{T}_{14}^+ + 18\widetilde{T}_{1N}^+$
$\mathcal{C}_4^A$	$-(6\mathbb{1} + 3Z_1 Z_4 Z_5 Z_N) T_{23}^+ - (6Z_1 Z_4 + 3Z_3 Z_N) T_{25}^+ - (6Z_1 Z_2 + 3Z_5 Z_N) T_{34}^+$	$-9\widetilde{T}_{23}^+ - 9\widetilde{T}_{25}^+ - 9\widetilde{T}_{34}^+$
	$+2(\mathbb{1} + Z_1 Z_2 Z_4 Z_5) T_{36}^+ - (6\mathbb{1} + 3Z_1 Z_2 Z_3 Z_N) T_{45}^+ + 2(\mathbb{1} + Z_1 Z_2 Z_3 Z_4) T_{56}^+$	$+4\widetilde{T}_{36}^+ - 9\widetilde{T}_{45}^+ + 4\widetilde{T}_{56}^+$

For a commutator $\mathcal{C}_n$ to yield a nonzero contribution to the fidelity, the product of the operators $\mathcal{C}_k^A$ should be proportional to $Z_1 Z_N$, that is, it should evaluate to even powers of $T_{1N}^{\pm}$. Hence very few terms appearing in Eq. (24) actually contribute to the transfer fidelity F.

The geometric construction of $\mathcal{C}_n^A$ yields only the *XY* operators contained in each commutator, but it does not reflect the appearance of prefactors proportional to Z_j [due to the commutator in Eq. (22)] that are explicitly written out in Table I. Thus, the geometric construction gives a necessary condition for transport, but not a sufficient one.

The operators $\mathcal{C}_n^A$ describe the sum of walks over different paths: for example, in $\mathcal{C}_2^A$, $Z_2 Z_3 T_{1N}^+$ can be interpreted as the information packet reaching node N through path P_1 in Fig. 5(a), while $Z_4 Z_5 T_{1N}^+$ represents propagation via path P_2. These two terms could in principle contribute to the fidelity, as they contain T_{1N}^+. However, the additional path-dependent factors $\prod_k Z_k$ lead to a loss of fidelity. Transport through different paths yield different $\prod_k Z_k$ factors, resulting in a destructive "interference" effect. Note also that since different paths are weighted by different correlation factors, they cannot be canceled through some external control to recover the fidelity. In the following section we show how a modified Hamiltonian can *remove* this path conditioning and thus drive perfect transport. Note that the path-dependent factors are unimportant in the case of pure states as well, provided the states reside in the same excitation manifold [25,52,53].

B. Correlating quantum walks over $\mathcal{N}$: Modified *XY* Hamiltonian

To remove the path conditioning one should modify the Hamiltonian so that the Z_j term in the commutator Eq. (22) disappears. This can be done via a modified *XY* Hamiltonian

$$\widetilde{T}_{ij}^{\pm} = T_{ij}^{\pm} \prod_{i<u<j} Z_u \tag{25}$$

since it satisfies this condition:

$$[\widetilde{T}_{ij}^{+}, \widetilde{T}_{jk}^{\pm}] = -\widetilde{T}_{ik}^{\mp}, \quad [\widetilde{T}_{ij}^{+}, \widetilde{T}_{kl}^{+}] = 0. \tag{26}$$

These operators now depend on the number of nodes between i and j, thus introducing a *metric* in the spin space that distinguishes paths between the two nodes i and j. Note that when the network $\mathcal{N}$ is a simple linear chain with nearest-neighbor couplings, the modified Hamiltonian $\widetilde{T}_{ij}^{+}$ is equivalent to the bare *XY* Hamiltonian. The modification in Eq. (25) of the *XY* Hamiltonian could also be seen as mapping the spin system into a set of noninteracting fermions [54,55] via a Jordan-Wigner transformation [56,57], since $C_i = \prod_{u<i} Z_u S_i^+$ are operators that satisfy the usual fermionic anticommutation relationships. When these modified operators are employed in the network $\mathcal{N}$ of Fig. 5(a), the two paths P_1 and P_2 in Fig. 5(a) are *indistinguishable* or, equivalently, they become perfectly correlated (see Table I). In effect, the modified *XY* Hamiltonian drives the quantum walks over different paths through a *common* set of operators of **B**. This is shown in Fig. 6 for a simple Λ network consisting of two Λ paths.

The graphic construction used to calculate the transport over the network in Fig. 5 remains unchanged, except that now the red lines between two nodes denote modified flip-flops $\widetilde{T}_{ij}^{\pm}$ between them. Crucially there are *no* path-dependent prefactors and symmetric nodes in each path become *equivalent* in each

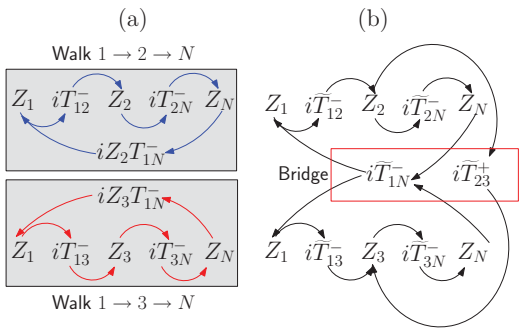

FIG. 6. (Color online) Operators appearing in the quantum walk of a network consisting of two Λ paths $1 \to 2 \to N$ and $1 \to 3 \to N$. In (a), where the transport is driven by the *XY* Hamiltonian, the two paths through spins 2 and 3 are different, as they traverse a different set of operators, and are thus depicted in two separated gray panels. In (b), where we consider the modified *XY* Hamiltonian, both walks go through a common set of operators. The previously separate walks are bridged by the operators in the red box, making the two walks indistinguishable and hence correlated.

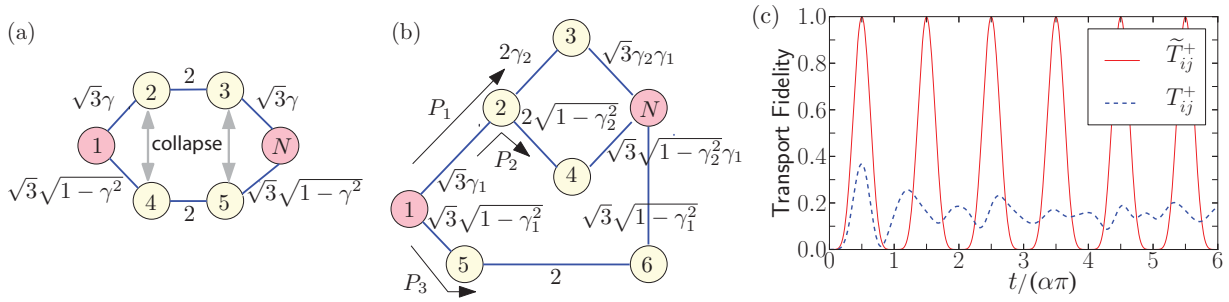

FIG. 7. (Color online) Engineered spin networks. (a) The network of Fig. 5(a), correlated by means of the modified flip-flop Hamiltonian, can be engineered to yield perfect transport by weighting the coupling strength α with the coefficient shown. Here γ is any positive parameter, $\gamma < 1$. The two paths P_1 and P_2 can be collapsed to form a linear chain, since nodes (2,4) and (3,5) are equivalent. (b) A more complicated network consisting of three paths P_1–P_3 (black arrows), with engineered strengths parameterized by $0 < \gamma_1, \gamma_2 < 1$. The three paths can be collapsed into an effective four-spin linear chain, with equivalent nodes (2,5) and (3,4,6). (c) Transport fidelity as a function of normalized time for the network in (b) with $\gamma_1 = 0.8, \gamma_2 = 0.5$, when the edges are the XY $\{T^{+}_{ij}\}$ or modified XY $\{\widetilde{T}^{+}_{ij}\}$ operators. In this last case perfect fidelity is achieved, while for the usual XY Hamiltonian the path-conditioned interference leads to poor transport fidelity.

of the operators $\mathcal{C}^{A}_{n}$. It is then possible to collapse different paths into a single effective one, until a complex network $\mathcal{N}$ is collapsed into a linear chain. This is depicted in Fig. 7(a).

We can express this result more formally, by defining *collapsed* XY operators, where we denote in parentheses equivalent nodes in two parallel paths:

$$\widetilde{T}^{\pm}_{i(j,k)} = \frac{1}{\sqrt{\gamma^2_{ij} + \gamma^2_{ik}}}(\gamma_{ij}\widetilde{T}^{\pm}_{ij} + \gamma_{ik}\widetilde{T}^{\pm}_{ik}), \tag{27}$$

where γ_{ij} and γ_{ik} are arbitrary parameters, $0 < \gamma_{ij}, \gamma_{ik} < 1$ (see also Appendix B). Remarkably, these operators satisfy the same path-independent commutation relations as in Eq. (26),

$$[\widetilde{T}^{+}_{i(j,k)}, \widetilde{T}^{\pm}_{(j,k)\ell}] = -\widetilde{T}^{\mp}_{i\ell}, \tag{28}$$

thus showing that intermediate equivalent nodes can be neglected in higher-order commutators. In addition the nested commutators $\mathcal{C}^{A}_{n}$ and the graphical method to construct them (Fig. 4) remain invariant when the modified XY operator is substituted with the collapsed operators $\widetilde{T}^{\pm}_{i(j,k)}$.

Using the collapsed operators, the network of Fig. 5(a) can thus be reduced to a simpler linear chain (Fig. 7). Analogous arguments for path collapsing were presented in Ref. [58] and have been applied before to some classes of graphs

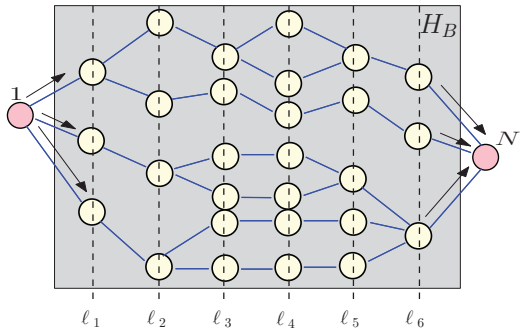

FIG. 8. (Color online) A complex network topology that can be engineered for perfect transport with the modified XY Hamiltonian. Collapsing the equivalent nodes along the lines ℓ_2–ℓ_5 leads to three equivalent paths that can be suitably engineered for perfect transport.

[9,38]. In the following we show that path equivalence could be constructed even for more complex network topologies, since, as we described, path collapse can be derived just from the commutation relationships between the edges of the network.

C. Engineered spin networks

The path collapse described in the previous section provides a constructive way to build networks, with appropriate coupling geometries and strengths, that achieve perfect transport. Alternatively, given a certain network geometry, the method determines all the possible coupling-strength distributions that leave its transport fidelity unchanged.

For example, starting from a linear chain, any node can be substituted by two equivalent nodes, thus giving rise to two equivalent paths. Then, within the subspace of the equivalent nodes, the couplings can be set using Eq. (27) with arbitrary weights γ, thus giving much flexibility in the final allowed network. The engineered network corresponding to Fig. 5(a) is represented in Fig. 7(a), where equivalent nodes from P_1 are weighted by γ, while those from P_2 are weighted by $\sqrt{1-\gamma^2}$.

A more complex example is shown in Fig. 7(b), where the network is built combining the networks in Figs. 3(a) and 5(a). It consists of three paths and can be collapsed into a four-spin linear chain. The couplings shown lead to perfect $Z_1 \to Z_N$ transport for arbitrary path weights γ_1 and γ_2, with $0 < \gamma_1, \gamma_2 < 1$, as shown in Fig. 7(c). The network engineering scheme can be recursively integrated to construct larger and more complicated network topologies (see, for example, Fig. 8).

Similar weighted networks have been considered before for bosons [36]. The engineered couplings derived by mapping quantum walks of N spinor bosons to the walk of a single particle are, however, much more restricted than what we found here via the mapping of spins to noninteracting fermions.

V. CONCLUSIONS AND OUTLOOK

Experimental implementation of quantum-information transport requires relaxing many of the assumptions made in ideal schemes. In this paper we analyzed a physical situation

that is closer to experimental settings—information transport in mixed-state spin networks with complex topologies. We first derived general conditions on propagators that allow perfect transport in these mixed-state spin networks. We used the conditions on the propagators to show that there exist classes of symmetry transformations on the Hamiltonians driving the transport for which the transport fidelity is invariant. We also showed that the propagator conditions imply that transporting some mixed states requires fewer control requirements than pure-state transport, an added advantage to using mixed-state channels in quantum-information architectures.

In order to study quantum transfer in complex spin networks, we described the dynamics as a continuous quantum walk over the possible paths offered by the network. This description provided a graphical construction to predict the system evolution, which highlighted the need to correlate the transport processes occurring along different paths of the network to obtain perfect transport. We thus introduced a modified *XY* Hamiltonian, based on Jordan-Wigner fermionization, that achieves correlation among paths by establishing a metric for the quantum walks occurring on the network. Conversely, the graphical construction could be used as well to study the generation from the usual *XY* Hamiltonian of states of interest in measurement-based quantum computation [59].

Finally, the quantum-walk picture and the graphical construction led us to define a constructive method to build complex networks from simpler ones, with appropriate coupling geometries and strengths, that achieve perfect transport. We thus found that there is considerable freedom in the choice of topology and interaction strength that still allows perfect transport in complex networks. While the requirement of a well-defined network topology could be further relaxed [60], the precise construction proposed in this paper would provide faster transport and the freedom in the coupling distributions could make these networks implementable in experimental systems.

ACKNOWLEDGMENT

This work was partially funded by NSF under Grant No. DMG-1005926.

APPENDIX A: CONSTRUCTING PERFECT TRANSPORT UNITARIES

Here we show how the conditions specified in Eq. (10) could be used to construct perfect transport propagators. Our motivation for this is to demonstrate that the conditions of Eq. (10) are very *weak*, in the sense that is possible to construct an infinite classes of unitaries that support $Z_1 \to Z_N$ transport.

Consider the matrix forms of $\hat{P}^{\mathcal{G}}_{Z_1Z_N}$ and $\hat{P}^{\widetilde{\mathcal{G}}}_{Z_1Z_N}$ in the two-dimensional $\{1,N\}$ subspace of $\mathcal{G}$ and $\widetilde{\mathcal{G}}$:

$$\begin{aligned}\mathcal{G} &\sim \{\{\mathbb{1},Z_1Z_N\},\{Z_1,Z_N\},\{X_1,Y_1Z_N\},\{Y_1,X_1Z_N\}\}\\ \widetilde{\mathcal{G}} &\sim \{\{X_1X_N,Y_1Y_N\},\{X_1Y_N,Y_1X_N\},\{X_N,Z_1Y_N\},\\ &\quad \{Y_N,Z_1X_N\}\},\end{aligned} \tag{A1}$$

where the $\sim$ refers to the restriction in the $\{1,N\}$ subspace. Then, for this order of basis, the matrix forms are block diagonal:

$$\begin{aligned}\hat{P}^{\mathcal{G}}_{Z_1Z_N} &= \mathrm{diag}([X,X,-Y,Y]),\\ \hat{P}^{\widetilde{\mathcal{G}}}_{Z_1Z_N} &= \mathrm{diag}([-X,X,-Y,Y]),\end{aligned} \tag{A2}$$

where X and Y are the standard Pauli matrices, whose eigenvectors with eigenvalues ± 1 are respectively $[1,\pm 1]^T$ and $[1,\pm i]^T$; this imposes a restriction on U. If $B_{\mathrm{bulk}}, B'_{\mathrm{bulk}} \in \mathrm{span}\{\mathbf{B}_{\mathrm{bulk}}\}$, one can explicitly list from Eq. (10) possible forms of U for perfect transport:

$$\begin{aligned}U_1 &= B_{\mathrm{bulk}}(\mathbb{1} \pm Z_1Z_N) + B'_{\mathrm{bulk}}(X_1X_N \pm Y_1Y_N),\\ U_2 &= B_{\mathrm{bulk}}(\mathbb{1} \pm Z_1Z_N) + B'_{\mathrm{bulk}}(X_1Y_N \mp Y_1X_N),\\ U_3 &= B_{\mathrm{bulk}}(Z_1 \pm \mathbb{1}Z_N) + B'_{\mathrm{bulk}}(X_1X_N \pm Y_1Y_N),\\ U_4 &= B_{\mathrm{bulk}}(Z_1 \pm Z_N) + B'_{\mathrm{bulk}}(X_1Y_N \mp Y_1X_N),\\ U_5 &= B_{\mathrm{bulk}}(X_1 \pm iY_1Z_N) + B'_{\mathrm{bulk}}(X_N \mp iZ_1Y_N),\\ U_6 &= B_{\mathrm{bulk}}(X_1 \pm iY_1Z_N) + B'_{\mathrm{bulk}}(Y_N \pm iZ_1X_N),\\ U_7 &= B_{\mathrm{bulk}}(Y_1 \pm iX_1Z_N) + B'_{\mathrm{bulk}}(X_N \pm iZ_1Y_N),\\ U_8 &= B_{\mathrm{bulk}}(Y_1 \pm iX_1Z_N) + B'_{\mathrm{bulk}}(Y_N \mp iZ_1X_N).\end{aligned} \tag{A3}$$

Note that the bulk of the network specified by B_{bulk} and B'_{bulk} can be any arbitrary operators with equal norm. In fact, the invariance described in Sec. III B could be used to show that the eight forms of U in Eq. (A3) are equivalent to U_1 or U_2.

Of course, one can combine the forms in Eq. (A3) to form other propagators that continue to support perfect transport. Consider, for example, a propagator constructed out of U_1 and U_2 in Eq. (A3), with $B_{\mathrm{bulk}}, B'_{\mathrm{bulk}} = \mathbb{1}$,

$$\begin{aligned}U &= \lambda_1(1 \pm Z_1Z_N) + \lambda_2(X_1X_N \pm Y_1Y_N)\\ &\quad + \lambda_3(X_1Y_N \mp Y_1X_N),\end{aligned}$$

where λ_j are coefficients to be determined. Then, from Eq. (4) we have

$$\begin{aligned}\langle U|U\rangle = 1 &\Rightarrow |\lambda_1|^2 + |\lambda_2|^2 + |\lambda_3|^2 = 1,\\ \langle U|\hat{P}_{Z_1Z_N}|U\rangle = 0 &\Rightarrow |\lambda_1|^2 = |\lambda_2|^2 + |\lambda_3|^2,\\ \langle U|\hat{P}_{Z_N}|U\rangle = 0 &\Rightarrow \mathrm{Im}(\lambda_2^*\lambda_3) = 0.\end{aligned} \tag{A4}$$

Other conditions in Eq. (4) are satisifed trivially. Equation (A4) can be solved exactly; for example, $\lambda_j = \{1/\sqrt{2},1/2,1/2\}$ is a solution. Importantly, however, if the B'_{bulk}'s are different for U_1 and U_2, the set of equations (A4) becomes far simpler.

In summary, achieving $Z_1 \to Z_N$ transport requires weak conditions on the propagator driving the transport. This is as opposed to perfect pure state transport, which requires the propagators to be isomorphic to permutation operators [31] that are mirror symmetric [45] about the end spins of the network.

APPENDIX B: PROPERTIES OF FLIP-FLOP AND DOUBLE-QUANTUM HAMILTONIANS

In this Appendix, we present simple relations satisfied by the flip-flop (*XY*) operators that are used in the main paper. Note that the double-quantum (DQ) operators in Eq. (14) follow analogous equations. In what follows, distinct indices label distinct spins in the network unless otherwise specified. We start with the definition of the operators

S and E:

$$E_j^{\pm} = \tfrac{1}{2}(\mathbb{1} \pm Z_j), \quad S_j^{\pm} = \tfrac{1}{2}(X_j \pm iY_j). \tag{B1}$$

These operators satisfy the following product rules:

$$\begin{aligned} &Z_j S_j^{\pm} = \pm S_j^{\pm}, \quad (S_j^{\pm})^2 = E_j^{\pm} E_j^{\mp} = 0, \\ &S_j^{\pm} S_j^{\mp} = (E_j^{\pm})^2 = E_j^{\pm}. \end{aligned} \tag{B2}$$

We define the flip-flop operators $T_{ij}^{\pm}$ and $L_{ij}^{\pm}$:

$$T_{ij}^{\pm} = (S_i^{+} S_j^{-} \pm S_i^{-} S_j^{+}), \quad L_{ij}^{\pm} = (E_i^{+} E_j^{-} \pm E_i^{-} E_j^{+}). \tag{B3}$$

From the definition in Eq. (B3) it follows that

$$T_{ij}^{\pm} = \pm T_{ji}^{\pm}, \quad Z_j T_{ij}^{+} = T_{ij}^{-}.$$

We have then the following product relations:

$$\begin{aligned} &(T_{ij}^{\pm})^2 = \pm L_{ij}^{+}, \quad T_{ij}^{\pm} L_{ij}^{+} = L_{ij}^{\pm} T_{ij}^{+} = T_{ij}^{\pm}, \\ &(L_{ij}^{\pm})^2 = L_{ij}^{+}, \quad T_{ij}^{\pm} T_{jk}^{+} = \tfrac{1}{2}(T_{ik}^{\pm} - Z_j T_{ik}^{\mp}) \end{aligned} \tag{B4}$$

and the commutation relations:

$$\begin{aligned} &[T_{ij}^{+}, T_{jk}^{+}] = -Z_j T_{ik}^{-}, \quad [T_{ij}^{+}, Z_j T_{ik}^{+}] = T_{kj}^{-}, \\ &[T_{ij}^{+}, Z_i] = -2T_{ij}^{-}, \quad [T_{ij}^{-}, Z_i] = -2T_{ij}^{+}. \end{aligned} \tag{B5}$$

We define the *modified* flip-flop operators $\widetilde{T}_{ij}^{\pm}$,

$$\widetilde{T}_{ij}^{\pm} = T_{ij}^{\pm} \prod_{i<u<j} Z_u, \tag{B6}$$

obtained by multiplying the flip-flop operator in Eq. (B3) by a factor of Z_u for all nodes between i and j. The modified flip-flop operators follow especially simple commutation rules:

$$[\widetilde{T}_{ij}^{+}, \widetilde{T}_{jk}^{\pm}] = -\widetilde{T}_{ik}^{\mp}, \quad [\widetilde{T}_{ij}^{+}, \widetilde{T}_{k\ell}^{\pm}] = 0. \tag{B7}$$

Note that, crucially, these commutators depend only on the initial and final nodes (i and k) and are independent of intermediate nodes. In a physical analogy, the modified operators $\widetilde{T}_{ij}^{+}$ behave as if they were *path independent*. Thus, when considering two (or more) paths, we could omit any intermediate node, since it would not enter in the ensuing commutators. We then denote *equivalent* nodes in parentheses—for example, (j,k) means that nodes j and k are equivalent—and define the *collapsed* operators:

$$\widetilde{T}_{i(j,k)}^{\pm} = \frac{1}{\sqrt{\gamma_{ij}^2 + \gamma_{ik}^2}} (\gamma_{ij} \widetilde{T}_{ij}^{\pm} + \gamma_{ik} \widetilde{T}_{ik}^{\pm}), \tag{B8}$$

where γ_{ij}, γ_{ik} are arbitrary parameters, $0 < \gamma_{ij}, \gamma_{ik} < 1$. The collapsed operators satisfy commutation relations similar to Eq. (B7):

$$\begin{aligned} &[\widetilde{T}_{i(j,k)}^{+}, \widetilde{T}_{(j,k)\ell}^{\pm}] = -\widetilde{T}_{i\ell}^{\mp}, \ [\widetilde{T}_{(j,k)i}^{+}, \widetilde{T}_{i\ell}^{\pm}] = -\widetilde{T}_{(j,k)\ell}^{\mp}, \\ &[\widetilde{T}_{(j,k)i}^{+}, \widetilde{T}_{i(m,n)}^{\pm}] = -\widetilde{T}_{(j,k)(m,n)}^{\mp}. \end{aligned} \tag{B9}$$

The collapsed operators in Eq. (B8) can be generalized. If $\mathbf{I} = (a_1, a_2, \ldots, a_m)$ and $\mathbf{J} = (b_1, b_2, \ldots, b_n)$ denote two sets of equivalent nodes, we have the collapsed operator

$$\widetilde{T}_{\mathbf{IJ}}^{\pm} = \frac{1}{\sqrt{\sum_{i=1}^{m} \sum_{j=1}^{n} \gamma_{a_i b_j}^2}} \sum_{i=1}^{m} \sum_{j=1}^{n} \gamma_{a_i b_j} \widetilde{T}_{a_i b_j}^{\pm}, \tag{B10}$$

which satisfies the commutation relationships

$$[\widetilde{T}_{\mathbf{IJ}}^{+}, \widetilde{T}_{\mathbf{JK}}^{\pm}] = -\widetilde{T}_{\mathbf{IK}}^{\mp}, \ [\widetilde{T}_{\mathbf{IJ}}^{+}, \widetilde{T}_{\mathbf{KL}}^{\pm}] = 0. \tag{B11}$$

[1] T. D. Ladd, F. Jelezko, R. Laflamme, Y. Nakamura, C. Monroe, and J. L. O'Brien, Nature (London) **464**, 45 (2010).
[2] J. I. Cirac, A. K. Ekert, S. F. Huelga, and C. Macchiavello, Phys. Rev. A **59**, 4249 (1999).
[3] D. K. L. Oi, S. J. Devitt, and L. C. L. Hollenberg, Phys. Rev. A **74**, 052313 (2006).
[4] L. Jiang, J. M. Taylor, A. S. Sorensen, and M. D. Lukin, Phys. Rev. A **76**, 062323 (2007).
[5] H. J. Kimble, Nature (London) **453**, 1023 (2008).
[6] R. V. Meter, W. J. Munro, K. Nemoto, and K. M. Itoh, J. Emerging Technol. Comput. Syst. **3**, 2:1 (2008).
[7] S. Bose, Phys. Rev. Lett. **91**, 207901 (2003).
[8] A. Kay, Int. J. Quantum. Inf. **8**, 641 (2010).
[9] M. Christandl, N. Datta, A. Ekert, and A. J. Landahl, Phys. Rev. Lett. **92**, 187902 (2004).
[10] C. Albanese, M. Christandl, N. Datta, and A. Ekert, Phys. Rev. Lett. **93**, 230502 (2004).
[11] G. M. Nikolopoulos, D. Petrosyan, and P. Lambropoulos, J. Phys.: Condens. Matter **16**, 4991 (2004).
[12] G. M. Nikolopoulos, D. Petrosyan, and P. Lambropoulos, Europhys. Lett. **65**, 297 (2004).
[13] G. Gualdi, V. Kostak, I. Marzoli, and P. Tombesi, Phys. Rev. A **78**, 022325 (2008).
[14] A. Wojcik, T. Luczak, P. Kurzynski, A. Grudka, T. Gdala, and M. Bednarska, Phys. Rev. A **72**, 034303 (2005).
[15] Y. Li, T. Shi, B. Chen, Z. Song, and C.-P. Sun, Phys. Rev. A **71**, 022301 (2005).
[16] Y. Wang, F. Shuang, and H. Rabitz, Phys. Rev. A **84**, 012307 (2011).
[17] D. Burgarth and S. Bose, Phys. Rev. A **71**, 052315 (2005).
[18] G. A. Álvarez, M. Mishkovsky, E. P. Danieli, P. R. Levstein, H. M. Pastawski, and L. Frydman, Phys. Rev. A **81**, 060302 (2010).
[19] J. Fitzsimons and J. Twamley, Phys. Rev. Lett. **97**, 090502 (2006).
[20] D. Burgarth, V. Giovannetti, and S. Bose, Phys. Rev. A **75**, 062327 (2007).
[21] T. Caneva, M. Murphy, T. Calarco, R. Fazio, S. Montangero, V. Giovannetti, and G. E. Santoro, Phys. Rev. Lett. **103**, 240501 (2009).
[22] D. Burgarth, K. Maruyama, M. Murphy, S. Montangero, T. Calarco, F. Nori, and M. B. Plenio, Phys. Rev. A **81**, 040303 (2010).
[23] P. Cappellaro, C. Ramanathan, and D. G. Cory, Phys. Rev. Lett. **99**, 250506 (2007).
[24] C. DiFranco, M. Paternostro, and M. S. Kim, Phys. Rev. Lett. **101**, 230502 (2008).

[25] P. Cappellaro, L. Viola, and C. Ramanathan, Phys. Rev. A **83**, 032304 (2011).
[26] N. Y. Yao, L. Jiang, A. V. Gorshkov, Z.-X. Gong, A. Zhai, L.-M. Duan, and M. D. Lukin, Phys. Rev. Lett. **106**, 040505 (2011).
[27] G. Kaur and P. Cappellaro, e-print arXiv:1112.0459.
[28] G. Panitchayangkoon, D. V. Voronine, D. Abramavicius, J. R. Caram, N. H. C. Lewis, S. Mukamel, and G. S. Engel, Proc. Natl. Acad. Sci. USA **108**, 20908 (2011).
[29] G. S. Engel, T. R. Calhoun, E. L. Read, T.-K. Ahn, T. Mancal, Y.-C. Cheng, R. E. Blankenship, and G. R. Fleming, Nature (London) **446**, 782 (2007).
[30] M. Mohseni, P. Rebentrost, S. Lloyd, and A. Aspuru-Guzik, J. Chem. Phys. **129**, 174106 (2008).
[31] V. Kostak, G. M. Nikolopoulos, and I. Jex, Phys. Rev. A **75**, 042319 (2007).
[32] Y. Aharonov, L. Davidovich, and N. Zagury, Phys. Rev. A **48**, 1687 (1993).
[33] J. Baum, M. Munowitz, A. N. Garroway, and A. Pines, J. Chem. Phys. **83**, 2015 (1985).
[34] M. Munowitz, A. Pines, and M. Mehring, J. Chem. Phys. **86**, 3172 (1987).
[35] O. Mlken and A. Blumen, Phys. Rep. **502**, 37 (2011).
[36] D. L. Feder, Phys. Rev. Lett. **97**, 180502 (2006).
[37] H. Krovi and T. A. Brun, Phys. Rev. A **75**, 062332 (2007).
[38] A. Bernasconi, C. Godsil, and S. Severini, Phys. Rev. A **78**, 052320 (2008).
[39] P. J. Pemberton-Ross and A. Kay, Phys. Rev. Lett. **106**, 020503 (2011).
[40] T. J. Osborne and N. Linden, Phys. Rev. A **69**, 052315 (2004).
[41] M.-H. Yung, Phys. Rev. A **74**, 030303 (2006).
[42] H. J. Cho, T. D. Ladd, J. Baugh, D. G. Cory, and C. Ramanathan, Phys. Rev. B **72**, 054427 (2005).
[43] O. Sorensen, G. Eich, M. Levitt, G. Bodenhausen, and R. Ernst, Prog. Nucl. Magn. Reson. Spectrosc. **16**, 163 (1984).
[44] A. Ajoy, R. K. Rao, A. Kumar, and P. Rungta, Phys. Rev. A **85**, 030303 (2012).
[45] P. Karbach and J. Stolze, Phys. Rev. A **72**, 030301 (2005).
[46] A. Kay, Phys. Rev. A **84**, 022337 (2011).
[47] I. N. Hincks, D. G. Cory, and C. Ramanathan, e-print arXiv:1111.0944.
[48] M. Markiewicz and M. Wiesniak, Phys. Rev. A **79**, 054304 (2009).
[49] S. C. Benjamin and S. Bose, Phys. Rev. Lett. **90**, 247901 (2003).
[50] S. R. Clark, C. M. Alves, and D. Jaksch, New J. Phys. **7**, 124 (2005).
[51] C. Di Franco, M. Paternostro, G. M. Palma, and M. S. Kim, Phys. Rev. A **76**, 042316 (2007).
[52] S. R. Clark, A. Klein, M. Bruderer, and D. Jaksch, New J. Phys. **9**, 202 (2007).
[53] C. Di Franco, M. Paternostro, and M. S. Kim, Phys. Rev. Lett. **102**, 187203 (2009).
[54] B. M. Terhal and D. P. DiVincenzo, Phys. Rev. A **65**, 032325 (2002).
[55] T. Barthel, C. Pineda, and J. Eisert, Phys. Rev. A **80**, 042333 (2009).
[56] P. Jordan and E. Wigner, Z. Phys. B **47**, 631 (1928).
[57] E. Lieb, T. Schultz, and D. Mattis, Ann. Phys. (NY) **16**, 407 (1961).
[58] A. M. Childs, Phys. Rev. Lett. **102**, 180501 (2009).
[59] R. Raussendorf, D. E. Browne, and H. J. Briegel, Phys. Rev. A **68**, 022312 (2003).
[60] A. Ajoy and P. Cappellaro (unpublished).